EVALUATION OF THE SUBSIDENCE BASED ON DINSAR AND GPS MEASUREMENTS NEAR KARVINÁ, CZECH REPUBLIC

PAVEL KADLEČÍK[1,2], VLASTIMIL KAJZAR[3], ZUZANA NEKVASILOVÁ[4], URS WEGMÜLLER[5], HANA DOLEŽALOVÁ[3]

[1] Institute of Rock Structure and Mechanics of the AS CR, v.v.i., Prague, Czech Republic
[2] Charles University in Prague, Faculty of Science, Department of Physical Geography and Geoecology, Czech Republic
[3] Institute of Geonics AS CR, v.v.i., Ostrava, Czech Republic
[4] Charles University in Prague, Faculty of Science, Institute of Geochemistry, Mineralogy and Mineral Resources, Czech Republic
[5] GAMMA Remote Sensing Research and Consulting AG, Gümlingen, Switzerland

ABSTRACT

The main impacts on the landscape due to coal mining in the Czech part of the Upper Silesian basin are ground subsidence and man-made landscape changes related to the mining. Two measurement techniques were used to determine the values of subsidence; these were then compared together to verify the results obtained. The first, differential SAR interferometry (dInSAR), a remote sensing method, was applied by Gamma Remote Sensing in the frame of ESA GMES Project Terrafirma, using ALOS PALSAR data. The second was the GPS fast static method, which was provided by the Institute of Geonics AS CR. The GPS monitoring was established at a locality near Karviná in 2006. A comparison of the results is described on one subsidence depression created above a panel mined from February 2007 to May 2008. Aspects of the comparison applying to the subsidence measurements are discussed along with the advantages and disadvantages of both methods.

Keywords: InSAR, GPS, subsidence, Karviná region, undermining

1. Introduction

The landscape between the cities of Ostrava and Karviná in the Czech portion of the Upper Silesian basin is greatly affected by coal mining activities. Present-day mining activities are concentrated in the vicinity of the city Karviná, where the OKD mining company operates 7 mining areas within an area of approximately 80 km^2 (Figure 1).

One of the main consequences of mining is ground subsidence. When coal seam is extracted, the overlaying layers immediately above the coal seam are allowed to collapse into the goaf. This sagging of the layers progresses on to the rocks above them, and towards the surface. The extent of subsidence at the surface is wider than the extent of the mined panel, with the maximal subsidence in the centre. Progress in the mining is reflected in progression of a depression or trough created at the surface, which evolves dynamically in the direction of the mining works, and its structure has a round or oval shape. The greatest amounts of subsidence, reaching to more than one meter, often can occur up to one year after the beginning of mining, primarilly depending on the thickness of the coal seam being mined.

One of the methods for subsidence detection in undermined areas is the processing of radar satellite images (SAR) using differential SAR Interferometry (dInSAR) (e.g. Stowe, Wright 1997; Perski, Jura 1999). Compared to conventional terrestrial methods of measurement (GNSS, levelling), its advantages are: the time saved; the possibility of studying large areas; and the ability to look back in time thanks to data archives from several satellites.

In this article we present the results of dInSAR processing on an example from the Upper Silesian Basin, documented through the period from February 2007 to May 2008. These results were derived by Gamma Remote Sensing within the frame of ESA GMES Project Terrafirma, with which the Institute of Rock Structure and Mechanics AS CR was involved.

The PALSAR dInSAR analysis, discussed here, was done in the ESA GMES Project Terrafirma as a complement to a Persistent Scatterer Interferometry (PSI) analysis of ERS and ENVISAT ASAR data, which was done prior (Wegmüller et al. 2007). The PSI results clearly show the displacements in areas away from the active coal excavation where subsidence rates are only up to a few cm per year. No results were obtained for areas that are above as well as near the coal seams where excavations took place during the observation period. Therefore, the objectives of the PALSAR dInSAR analysis were on one hand to close these spatial gaps and to get displacement information in the faster moving areas as well as to demonstrate some monitoring capability (i.e. to show that strong temporal variations can be observed). PALSAR was selected because we expected a greater potential to achieve these objectives. Thanks to the longer L-band wavelength (PALSAR), the phase gradients from the displacements are reduced compared to the C-band (ERS, ENVISAT). Additionally to L-band, less decorrelation over vegetation is expected, resulting in better spatial coverage over rural areas.

In this work the quality and applicability of the dInSAR results are compared with the results of GNSS monitoring (using GPS satellites) from the locality near Karviná,

http://dx.doi.org/10.14712/23361980.2015.86
Kadlečík, P. – Kajzar, V. – Nekvasilová, Z. – Wegmüller, U. – Doležalová, H. (2015): Evaluation of the subsidence based on dinSAR and GPS measurements near Karviná, Czech Republic
AUC Geographica, 50, No. 1, pp. 51–61

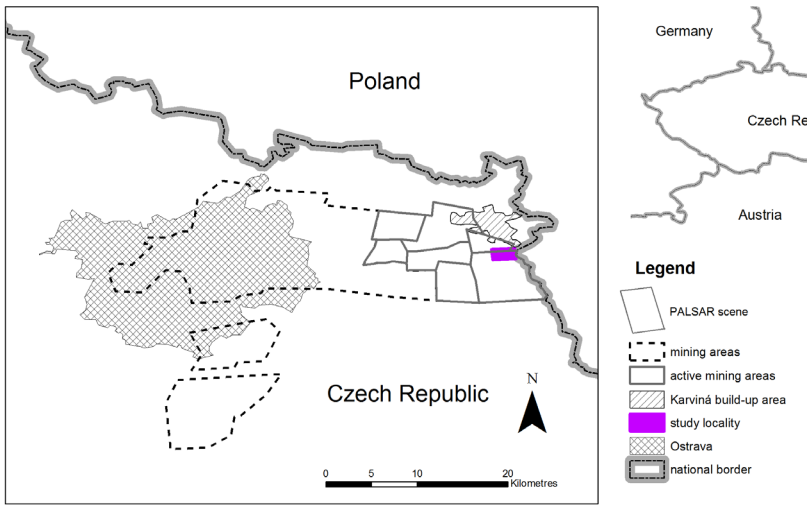

Fig. 1 Mining district in the Czech portion of the Upper Silesian Basin.

which has been under detailed study by researchers from the Institute of Geonics AS CR. A substantial aim and motivation for this research was also to supplement various recent studies on mining subsidence in the Czech portion of the Upper Silesian basin which have been presented until now (e.g. Schenk 2006, Kadlečík et al. 2010, Kajzar et al. 2011, Doležalová et al. 2012, Mulková, Popelková 2013, Lazecký, Jiránková 2013).

2. Differential Interferometry SAR

Differential Interferometry SAR (dInSAR), a remote sensing method, utilizes SAR (Synthetic Aperture Radar) images to determine changes of the Earth's surface. SAR images are acquired by satellites, which repeat their orbits over the same area with regular intervals (called repeat cycles). SAR images acquired by satellite SAR sensors contain information of both the amplitudes and the phases of the returning signal within the imaging area. The phase information of the signal can be used to determine the distance between the satellite and target on the surface along the line-of-sight (LOS).

Two SAR images, acquired at different times, can be combined to produce a interferogram. An interferogram, representing phase differences between the two acquisition, consists of information about topography (Φ_{topo}), surface changes in the line-of-sight direction (Φ_{def}), atmospheric disturbances (Φ_{atm}), orbit errors (Φ_{orbit}), and noise (Φ_{noise}):

$$\Delta\Phi = \Phi_{topo} + \Phi_{def} + \Phi_{atm} + \Phi_{orbit} + \Phi_{noise}$$

In order to acquire information about the displacement (Φ_{def}) between the two acquisitions, the other components of the phase are removed or minimalized. For a detailed description of the principle of dInSAR see e.g. Hanssen (2001), Cumming, Wong (2005), Fletcher et al. (2007). The widespread application of dInSAR is described in e.g. Massonet, Feigl (1997).

3. Differential SAR interferometry processing

For the Upper Silesian Basin seven PALSAR scenes (from the Japanese satellite ALOS), with both single (FBS) and dual (FBD) polarization modes (Table 1), were selected for the dInSAR processing. The ALOS satellite was operated until May 2011 with a repeat cycle of 46 days over the same area. The SAR scenes used were taken from an off-nadir angle of 34.3°.

Tab. 1 ALOS PALSAR data used for this study.

Date of SAR image	Pass	Track	Orbit	Polarization mode
22.2.2007	ascending	625	5759	FBS
10.7.2007	ascending	625	7772	FBD
25.8.2007	ascending	625	8443	FBD
25.11.2007	ascending	625	9785	FBD
25.2.2008	ascending	625	11127	FBS
27.5.2008	ascending	625	12469	FBD
12.7.2008	ascending	625	13140	FBD

All of the scenes were processed to single look complex images and then co-registered to the same slant-range geometry. For the processing of single interferometric PALSAR data pairs, a two-pass differential SAR interferometry approach was applied, using the SRTM 3" DEM as the height reference. As a special processing step, optimized for the fast deformation rates expected in the case of active mining and landslides, the localized deformation signal and the large scale error terms (large-scale atmospheric distortion and baseline-related phase errors) were separated, based upon their different spatial dimensions (Wegmüller et al. 2007). The methodology used in the case of mixed FBS and FBD pairs is described in greater detail in Werner et al. (2007).

The processing was then completed by phase unwrapping, and the subsequent conversion of the unwrapped

phases to vertical deformation values (Table 2). Phase unwrapping was quite critical in some parts of the interferograms (low coherence, and relatively high-phase gradients), especially in the case of the 1st period (138 days). Additionally, we should note that one other pair of images was processed (from 27. 5. 2008 to 12. 7. 2008 – 46 days); however, phase unwrapping was not computed because of the very long perpendicular baseline (Bperp = 3856 m) for this interval, meaning that no subsidence values were obtained. Therefore, this period is not included in further analysis (comparisons).

Tab. 2 dInSAR processed periods for comparison with GPS.

Period	date of 1st image	date of 2nd image	time interval	Bperp
1st	22.2.2007	10.7.2007	138 days	809 m
2nd	10.7.2007	25.8.2007	46 days	235 m
3rd	25.8.2007	25.11.2007	92 days	740 m
4th	25.11.2007	25.2.2008	92 days	1189 m
5th	25.2.2008	27.5.2008	92 days	424 m

It is important to note that information about ground displacement from dInSAR processing is along the line-of-sight (LOS). The LOS displacement values were converted to vertical displacement values by assuming that the displacement was strictly in the vertical direction (which is not entirely correct). The underground extraction of coal, results in various movements, including: vertical subsidence, horizontal displacement, horizontal strains, as well as the curvature and tilting of the ground surface (Schenk 2006). The maximum vertical subsidence culminates at the center of the subsidence depression, where all other movements are at their minimum; therefore, at the center of the subsidence depression we can assume that the LOS displacement only consists of vertical subsidence. As well as on margins of a subsidence (where the movements decline to zero), it is possible to suppose the LOS displacement processed by dInSAR as a vertical subsidence. To compare and verify dInSAR results with the results of GPS monitoring (which records accurate horizontal and vertical positioning of points on the ground's surface), this is done by using only the GPS vertical component (simplified in Figure 3).

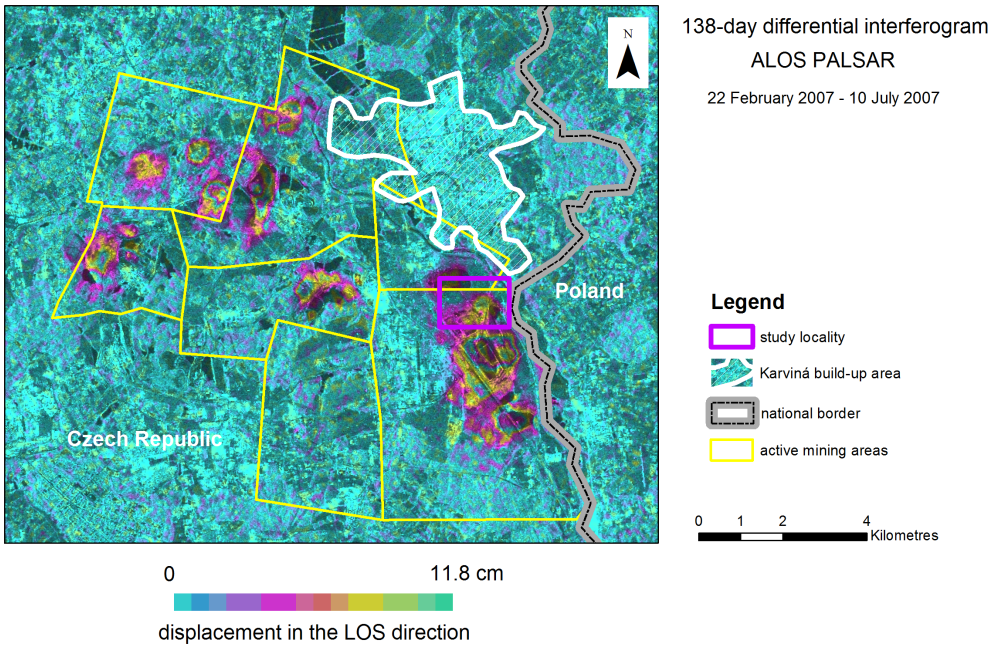

Fig. 2 Unwrapped differential interferogram for the 1st period in the active mining area of the Czech portion of the Upper Silesian Basin (coloured areas represent ground subsidence).

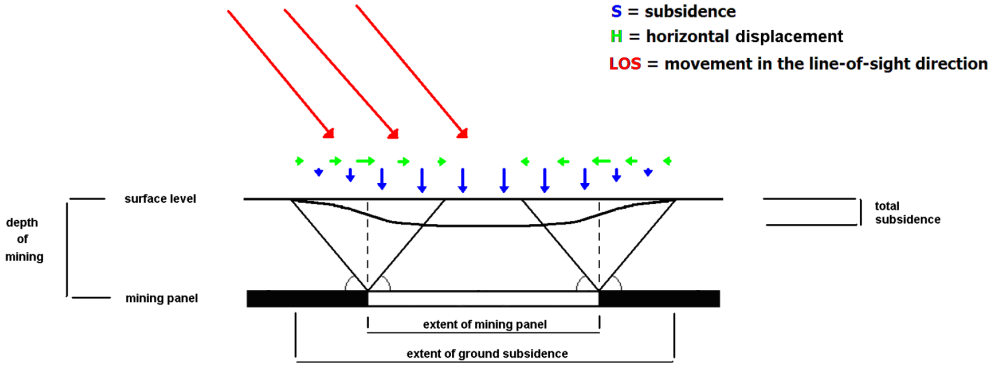

Fig. 3 Simplified chart of horizontal and vertical movements in subsidence depression related to LOS direction – illustrated subsidence depression according to Schenk (2006).

4. Monitoring of the subsidence depression using GPS

During 2007–2009, the Institute of Geonics AS CR was involved in a grant project (Czech Science Foundation No. 105/07/1586) the primary task of which was to monitor the development of the emerging subsidence basin in an area with active underground mining. The selected area is located in the Louky mining area (CSM mine) in the eastern portion of the Ostrava-Karvina coal district (Figure 1 and Figure 2). The eastern boundary is formed by the river Olza (Olše in Czech), creating a natural border there between the Czech Republic and Poland. The northern boundary is delimited by the Darkov mining area (Figure 4). The entire area belongs to the zero block, and the first block of the mining area is the CSM mine. The blocks are defined by tectonic disturbances, running approximately from the W-E and N-S directions (Dopita et al. 1997).

In the 1990s, the area of the zero block (CSM mine) was engaged in intense mining activities at the coalface. The impact of these mining activities on the surface was observed by precise levelling. By 2004, it could then be regarded as relatively stable ground, with an maximum annual subsidence of 5 cm (Kajzar 2012). Extraction at the coalface was renewed in October 2006. At that time, they began mining of coal face 361 000, lasting until June 2007. From May 2007 to April 2008 this was followed by the mining of coal face 293 102, south from the one previously, located in the first block of the CSM mine. Both coalfaces were mined in an east to the west direction by the longwall method. A detailed description of the deposit, the thickness of the extracted coal seam, method of exploitation, and tectonics can be found in Dolezalova et al. (2009).

The subsidence had a significant influence on changes of the relief in the study area; therefore, there is currently ongoing surface reclamation. Within the framework of these activities, there has been the deposition of mine waste rock at several places in the study area, although most of them were in the eastern portion. The west and north-west parts of this terrain are already in advanced stages of reclamation, i.e. grassing and the planting of vegetation.

About 100 observation points were constructed, with the aim being to monitor the development of the newly-emergent mining subsidence in this area (starting from 2006). These points are spread across the entire study area. They were surveyed approximately once per month by GNSS/GPS fast static methods (described e.g. in Skeen (2011)). Based on the data from individual measurements, it is possible to evaluate the vertical and horizontal movements in the area and generate time-spatial models describing the development of a nascent subsidence depression (Doležalová et al. 2010). Extraction from coalfaces 361 000 and 293 102 has resulted in an increase in the total subsidence, being greater than 1 m in some places (Doležalová et al. 2012; Kajzar, Doležalová 2013).

5. Process of comparison of dInSAR and GPS results

Comparisons of the results obtained from both dInSAR and GPS were carried out for 5 periods, determined by the dates of acquisition of input SAR images covering the study area (Table 2, Figure 4). These five periods coincide with the dates of extraction of coal faces 361 000 and 293 102. It should be noted that the excavation in the eastern part of the northern coal face (361 000) began before the first period, and the effects of that mining will certainly be evident in the evaluation.

By processing the dInSAR, we detected a displacement between the satellite and the surface, i.e. in the so-called

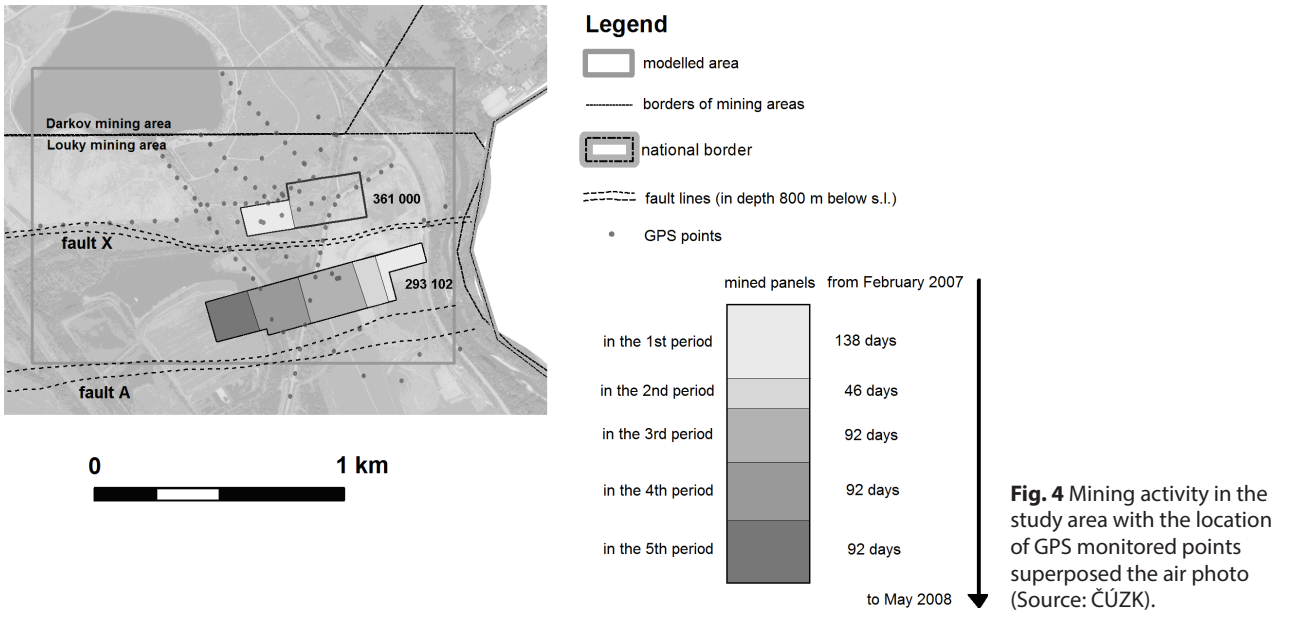

Fig. 4 Mining activity in the study area with the location of GPS monitored points superposed the air photo (Source: ČÚZK).

LOS direction, including possible horizontal and vertical components of movement (Figure 3). For comparison, the LOS values were converted into a vertical subsidence, neglecting any possible non-zero horizontal component. The subsidence value was estimated from the dInSAR results for each point measured by GPS, defined by its x and y coordinates. There is a partial generalization of the pixel value due to the limited resolution of dInSAR raster images (20 × 20 meters per pixel).

GPS measurements were performed approximately with a one month periodicity. Therefore, rarely did the time of the satellite imagery coincide with the time of the GPS measurements. From this standpoint, it was necessary to estimate the elevation of the monitored points relating to the dates of the SAR imaging. For this purpose, the linear interpolation method was chosen as an aid. Calculation of the elevation is dependent on the time factor. Using the linear interpolation method, the elevations of each GPS measurement point were defined corresponding to the day of SAR imaging. The subsidence of each individual point was calculated for each period.

This method of linear interpolation is considered to be suitable in those cases where there was a genuinely smooth development of the subsidence curves of most points (Staš et al. 2009). However, this approach cannot determine the true value of the subsidence. It is therefore necessary to establish a real interval, i.e. minimum and maximum possible value of subsidence for a given period, based on the actual GPS data. A simplified example of an complete calculation is demonstrated below (Figure 5).

The model of subsidence depressions was used for each period, using the geostatistical interpolation method of kriging of the GPS values. These were then compared with the results of the dInSAR processing, and also with the models based on the subsidence values for each GPS point taken from the dInSAR results (Figure 6, below).

In the last step, the subsidence curves were drawn from the evaluated data for dInSAR and GPS; demonstrating the development of subsidence of each point during the five monitored periods. In the case of dInSAR, there is a subsidence curve having a shape determined by the gradual accumulation of the determined values during the study period. The GPS subsidence curve has no basis in the gradual accumulation of values, but the subsidence curve is continually calculated from the values, based upon the actual measured data (as described prior). In addition, this subsidence curve is supplemented by error bars, which define the possible subsidence value with respect to a specific period (Figure 5 for error bar calculations).

6. Results of comparisons

The extent of the subsidence depression and the determination of its centre is evident from the comparison of the dInSAR processing and GPS models (Figure 6).

For the first two periods studied, it is possible to see a high degree of similarity between these models (i.e. the GPS model and dInSAR results during these particular periods). In the third and fourth period, the situation is different; thus there are varying degrees of difference of the compared models. In the case of the third period, the difference is most likely related to the spatial filtering and phase unwrapping procedure applied in the dInSAR processing. The shape of the subsidence depression makes it look like "a cake bitten into". The GPS model also shows a much bigger subsidence in the middle of the depression than does the dInSAR results (GPS 21 cm – dInSAR 13 cm). A more marked drop in the centre of the subsidence depression on the GPS model is also evident from a comparison of the fourth series models (GPS 39 cm – dInSAR 14 cm). For the last period, the greater part of the models couldn't be compared, because of the incomplete evaluation of the dInSAR results. The size and distribution of the subsidence in comparable parts of the models are very similar. The differences between the models which were created based upon GPS points, which had assigned values of the observed subsidence from dInSAR (Figure 6 – third row), and those models based on GPS measurements (Figure 6 – second row), are clearly visible; as in the previous comparisons. On the other hand, there are also obvious differences in comparison with the results of the dInSAR processing (Figure 6 – first row). Hence, it can be seen that the models which are created from a relatively small number of data points (and due to

Year - Week		2007-27	2007-28	2007-29	2007-30	2007-31	2007-32	2007-33	2007-34	2007-35	2007-36	2007-37	2007-38	2007-39	2007-40
Date (GPS measurement)		3.7.2007			26.7.2007				23.8.2007						2.10.2007
Date (SAR images)			10.7.2007							25.8.2007					
Subsidence for period (dInSAR)	cm									**3.3**					
Elevation (measured by GPS)	m.a.s.l.	276.253			276.234				276.228						276.197
Elevation (interpolated value)	m.a.s.l.		**276.247**							**276.227**					
Subsidence for period (GPS)	cm									**2.0**					
Subsidence (GPS - inner time interval)	cm									0.6					
Subsidence (GPS - outer time interval)	cm									5.6					

Fig. 5 An example of a calculation of the subsidence for 2nd period from the GPS data, sample point a06. (For the purpose of this example, the interpolation of the values is simplified into weeks.)

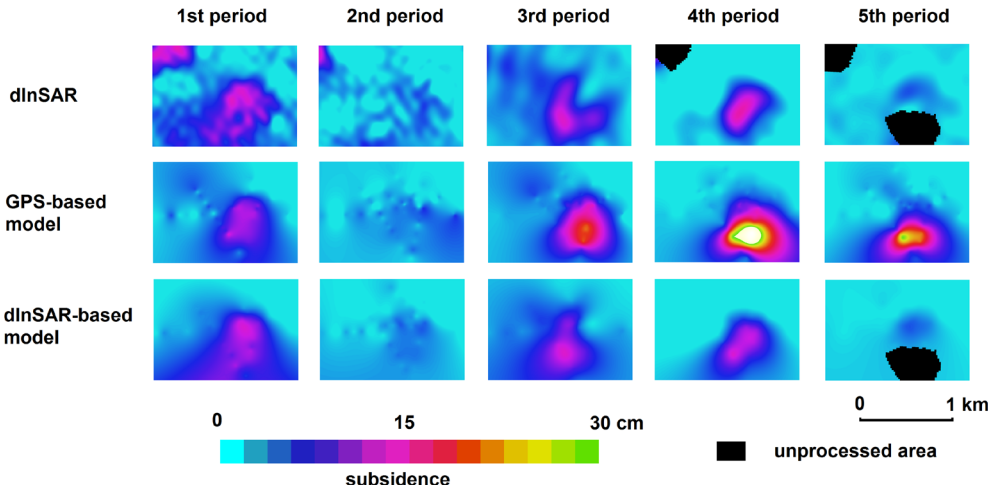

Fig. 6 Subsidence evolution based on dInSAR (top row), GPS (middle row), and subsidence values for GPS points obtained from dInSAR (bottom row) for the 1st to 5th period (from left to right).

their mutual positions) cannot fully and exactly express the developments in an area of interest.

By comparing the subsidence curves for each individual point, we reached two conclusions: (1) the curves mutually correspond, i.e. the dInSAR values match the values from the GPS, or are within the specified limits (Figure 7, left); (2) in the beginning the curves correspond, and then there is a subsequent breakdown of their comparable development. After the mutual divergence is usually observed, the same trend of subsidence in the rest of the curve continues, which could be an indication of incorrect dInSAR values in the proper sub-period (Figure 7, right).

If the dInSAR values are experimentally corrected in the positions of the deviation, they will more closely correspond with the course of the GPS curve (see example in Figure 8).

The next step was to find out, whether the specified dInSAR value belongs in the interval defined by the minimum and maximum possible values of subsidence for each period in the study period. There were points identified, in which the subsidence value obtained from dInSAR was significantly different from the value based on the GPS measurement in that particular period. This comparison is also possible to be done graphically (Figure 9).

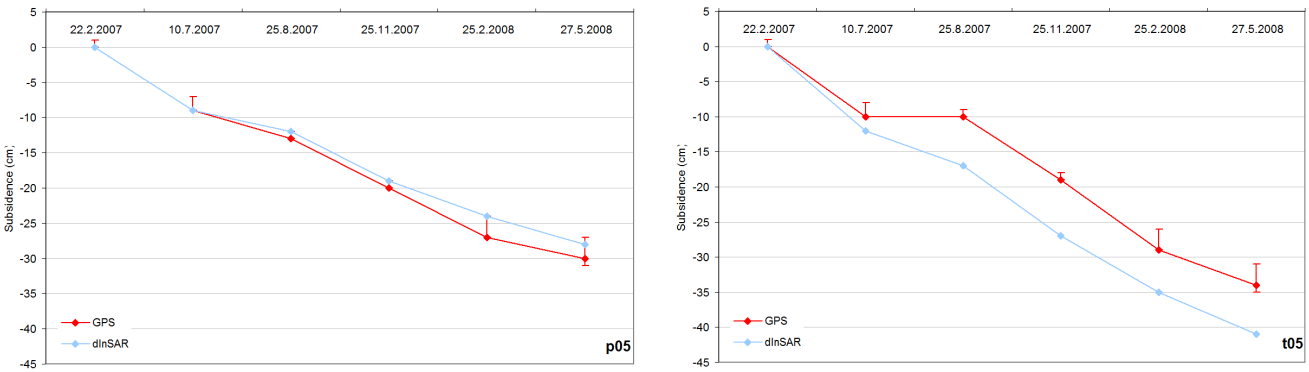

Fig. 7 Charts of the development of subsidence curves of the two selected points (GPS – red line, dInSAR – light blue line). The point on the left (p05) has a similar trend of subsidence for all periods; the point on the right (t05) has a different subsidence value in the second period.

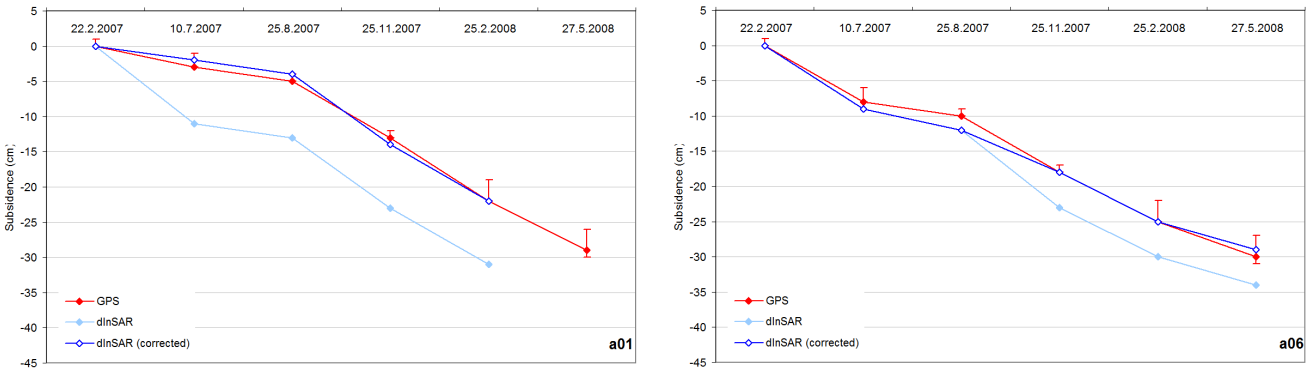

Fig. 8 An example of correction of the dInSAR subsidence curve in positions of deviation (GPS – red line, dInSAR – light blue line, "corrected dInSAR" – dark blue line). Values of subsidence are corrected in the 1st period (left chart) and 3rd period (right chart).

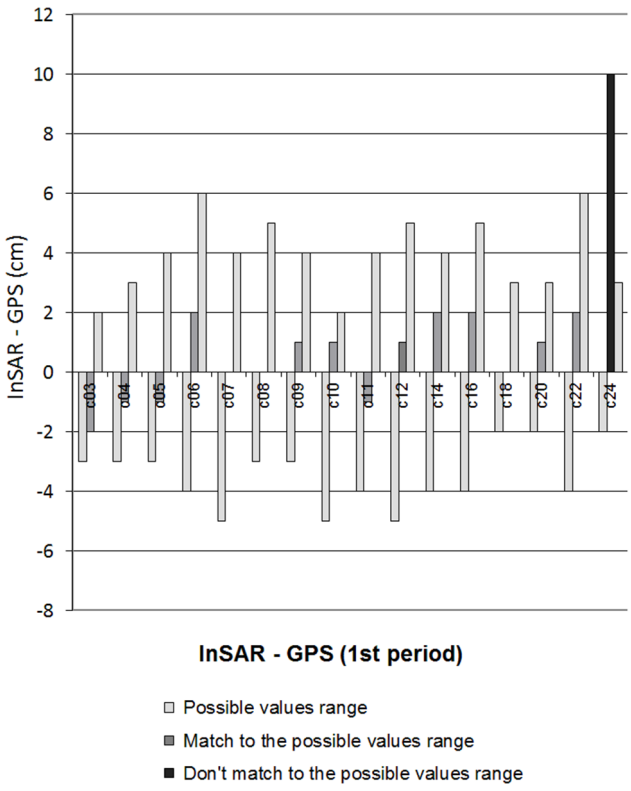

Fig. 9 Revealing incorrect values – graphical evaluation.

All points where errors have been found are highlighted in each period (Figure 10). Most of the highlighted points are located near the centre of the subsidence depression (3rd and 4th period), as well as to the west of it (1st and 3rd periods). They are located near each other. This may suggest that there is an error at that particular part of the interferogram. A statistical comparison of the subsidence values (dInSAR vs GPS) at each GPS-point for each period is displayed in Figure 11.

7. Discussion

Discrepancies were found when a comparison between both datasets was done. These discrepancies may be caused by:

- differences between dates when they were measured using GPS and the dates which had come from the SAR images;
- inaccuracies in georeferencing and the calculation of subsidence values from the 20 × 20 m grid (for comparison with GPS);
- errors related to the spatial filtering and unwrapping procedure applied in the dInSAR processing; and/or
- GPS measurement errors.

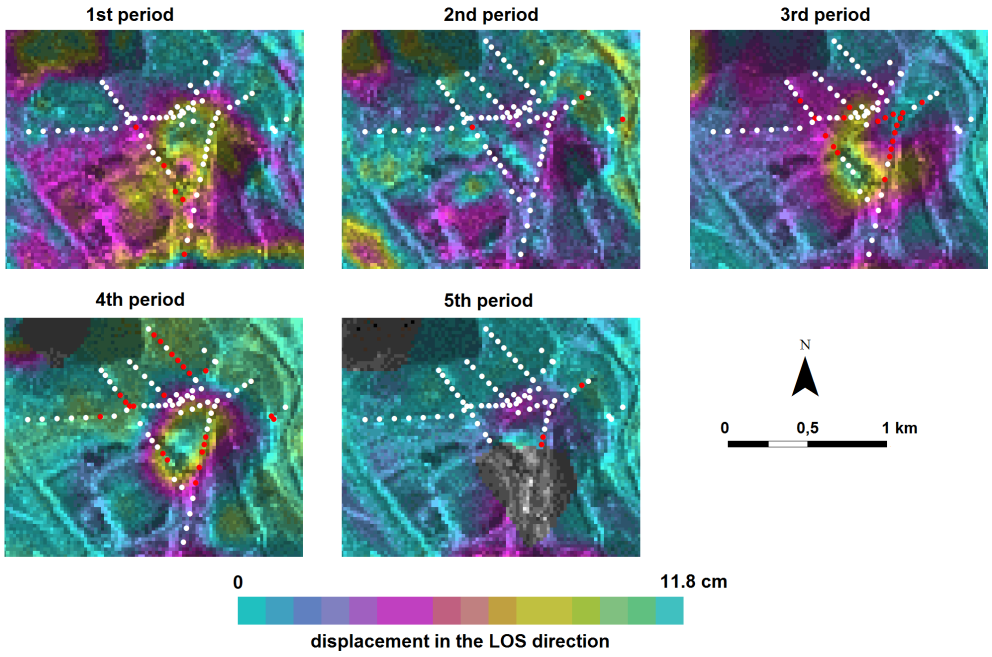

Fig. 10 Positions of problematic points superposed the unwrapped differential interferograms for each period. Dots represent all points measured by GPS in the study area; problematic points are coloured red.

	1st period	2nd period	3rd period	4th period	5th period
days	138	46	92	92	92
compared GPS-points	69	84	83	83	72
DIFF AVG (cm)	0.95	-0.21	-1.06	-3.95	-0.87
DIFF RMSE (cm)	2.20	1.68	5.26	6.77	2.54
DIFF IN INT	**64**	**81**	**64**	**61**	**69**
DIFF IN INT (%)	**92.8%**	**96.4%**	**77.1%**	**73.5%**	**95.8%**
DIFF IN 2CM	52	68	46	23	62
DIFF IN 2 CM (%)	75.4%	81.0%	55.4%	27.7%	86.1%

DIFF AVG – average of differences between compared values (GPS vs. dInSAR)
DIFF RMSE – root-mean-square error of differences between compared values (GPS vs. dInSAR)
DIFF IN INT – number of GPS-points with dInSAR values falls into real interval established by GPS measurements
DIFF IN 2CM – number of GPS-points with differences between compared values (GPS vs. dInSAR) up to 2 cm

Fig. 11 Statistics of compared subsidence values on GPS-points between dInSAR processing and GPS measurements. Statistics within the shaded rows are illustrated in Figure 10.

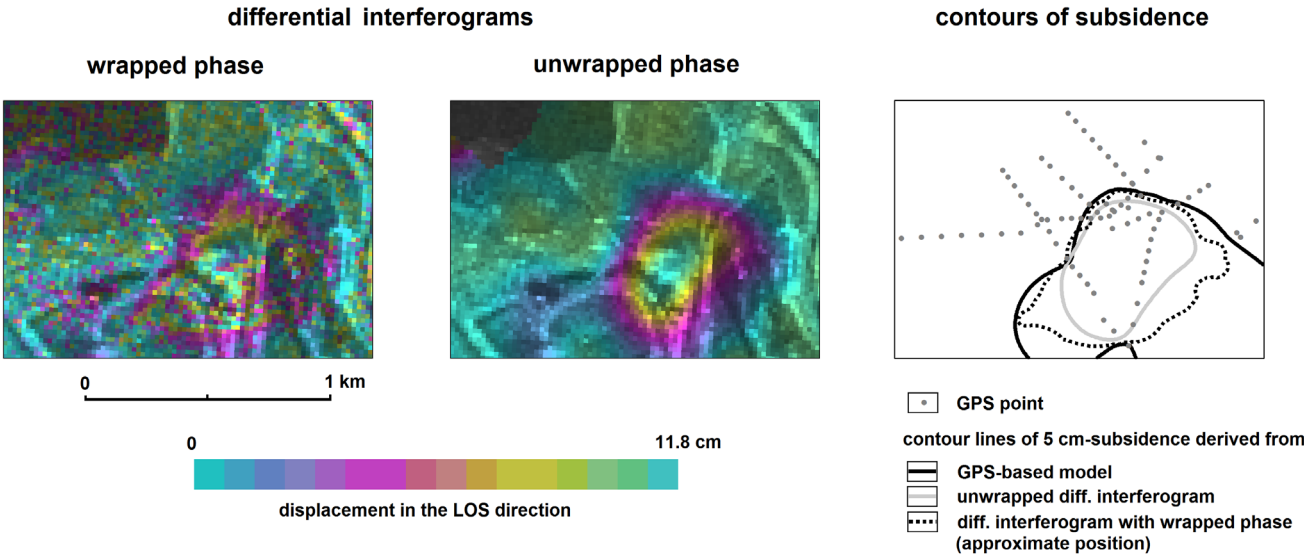

Fig. 12 Comparison of subsidence, derived from a differential interferogram before (left) and after unwrapping (middle). The righthand image shows the 5 cm contour lines of subsidence.

Errors caused by the differencies in the days of GPS measurements and the days of captured SAR images used for comparisons were solved by creating a tolerant border widening of each time period (defined by SAR image acquisitions) to the nearest GPS measurement. Inaccuracy in the georeferencing of the images and calculation of the subsidence values from the 20 × 20 m grid could affect the comparison values at these points; however, it does not affect the overall shape and position of the centre of the subsidence depression. These are probably caused by spatial filtering and the unwrapping procedure applied; mainly for the 3rd and 4th periods, when the spatial phase gradients present were particularly high. A possible way to detect these errors is to compare the interferogram before and after the unwrapping phase (Figure 12). On the other hand, the many correct values indicate that atmospheric path delay effects were clearly not the problem for the sharply deviating values.

Errors are present, particularly in those cases where very high phase gradients are usually present in the central parts of the subsidence depression, caused by a large subsidence drop in a relatively small area (with regard to the resolution of the input images). The quality of the dInSAR processing could also be affected by waste rock dumping and other adjustments within the reclamation field, which took place in the studied area during the study period (with respect of usage SRTM DEM from 2000). The different extent of the subsidence area (dInSAR vs. GPS-model) outwards from the centre of the subsidence trough is caused by the absence of a greater number of points serving as inputs for the GPS model. The same applies to determining the effects of subsidence in the surrounding areas in the NW and S, which was partially resolved by extending the number of GPS-measured points in subsequent years. Errors of individual GPS measurements extended to 1 cm, and are not reflected in the values of the total subsidence because they are measured as absolute altitudes. Theoretically, the introduction of GPS measurement errors would occur just before the first and the last period when plotting the values of tolerance.

8. Conclusion and future outlooks

By differential radar interferometry processing there were about 20 subsidence depressions detected in the Czech portion of the Upper Silesian basin between February 2007 and May 2008. One of the subsidence depressions in the locality near Karviná has been under detailed GPS monitoring from 2006 by researchers from the Institute of Geonics AS CR. For both excavation sites known to be active during the time period being considered, at least indications of significant subsidence are present in the dInSAR results. For the case investigated, overall the observed temporal behaviour corresponds well to the available GPS measurements. Periods with and without excavation activity can clearly be identified. So, in a qualitative sense, the objectives could be achieved.

The quantitative comparisons of the GPS and dInSAR subsidence values demonstrates the suitability for the application of these techniques in studies of undermined areas similar to the Karviná area. GPS measurements with subsequent modeling are a valuable source of information about subsidence processes in active coal mining areas. DInSAR allows for the identification of these changes retrospectively. The spatio-temporal evolution of the mining induced subsidence was described by evaluation of 5 consecutive time-periods. The analysis of the results from both techniques helped to determine the accuracy of dInSAR processing, as well as to detect anomalies caused by the applied spatial filtering and the unwrapping procedure errors in the dInSAR processing.

Assessing the dInSAR result in a quantitative sense shows that some information gaps still remain. In part, these gaps relate to areas where the phase unwrapping could not be resolved (see unprocessed areas on Figure 6); i.e., to areas with strong displacement gradients. Overall, in the processing we tried to find a reasonable compromise between achieving a good spatial coverage and the reliability of the deformation values derived. As the comparison with the detailed GPS measurements shows, this was partly successful in that very reasonable values are generally obtained. Nevertheless, as a consequence of the spatial filtering and unwrapping procedure used, there are also some values present which more significantly deviate from the GPS measurements.

Except for the rates of subsidence, it is possible by comparison (of GPS vs. dInSAR) to: (1) identify the extent of surface subsidence; (2) modify the spatial models (based on GPS data) describing the development of the subsidence area; and (3) determine additional undermined locations which were not of interest in the choices for GPS monitoring, but which could have influenced the subsidence in the studied location. In the case of dInSAR's application, it is necessary to know about events both under the surface (e.g. extent of mining works – past and present), as well as the situation on the surface (information about ongoing changes of the anthropogenic relief over undermined areas – waste dumps, landscape reclamation, etc.).

Nevertheless, for other applications of GPS and InSAR data it is necessary for a detailed quantification of the accuracy of dInSAR processing with the assistance of GPS (i.e. numerical and statistical comparisons of the subsidence values for each period), and the elimination of identified errors or inaccuracies in the comparisons (especially unwrapping procedure errors). This allows us to create a model of total subsidence from the dInSAR results for the period from February 2007 to May 2008, and its comparison with the GPS model created by the first and last measurements for that period. Supplementary dInSAR information on the subsidence values observed in the surroundings can improve the quality of the current GPS models. Another improvement could possibly be obtained by challenging current GPS models with models derived from dInSAR-subsidence values only at those points measured by GPS, as done in Figure 6.

Finally, the geomorphological monitoring of anthropogenic relief started on the surveyed area in the summer of 2011. The principal aim is to detect and describe recent changes of the relief in the active mining area with the support of supplementary elevation and air-photo data.

Acknowledgements

The dInSAR processing was supported by the ESA GMES Project Terrafirma No. 98042. Parts of the work were further supported by: the Charles University Grant Agency (Project GAUK No. 321011/PrF/B-GEO "Change of anthropogenic relief in the Ostrava basin", based on InSAR results); the Ministry of Education, Youth and Sports of the Czech Republic (Project No. LC506); and Project Institute of clean technologies for mining and utilization of raw materials for energy use – Sustainability program. Identification code: LO1406. Project is supported by the National Programme for Sustainability I (2013–2020) financed by the state budget of the Czech Republic. ALOS PALSAR data are courtesy of JAXA RA 094 (PI Urs Wegmüller). This work was carried out with the support of the long-term conceptual development research organisation RVO: 67985891.

REFERENCES

BUREL, F., CHODURA, A., FIALA, J., HEBELKA, J., JANÁK, J., RYŠAVÝ, J. (1991): Výpočet zásob černého uhlí Důl ČSM, s. p. Stonava, stav k 1. 1. 1991. ČGS Geofond, Praha.

CUMMING, I. G., WONG, F. H. (2005): Digital Processing of Synthetic Aperture Radar Data: Algorithms and Implementation. Artech House, 660p.

DOLEŽALOVÁ, H., KAJZAR, V., SOUČEK, K., STAŠ, L (2009): Evaluation of mining subsidence using GPS data. Acta Geodynamica et Geomaterialia 6(3), 359–367.

DOLEŽALOVÁ, H., KAJZAR, V., SOUČEK, K., STAŠ, L (2010): Evaluation of vertical and horizontal movements in the subsidence depression near Karviná. Acta Geodynamica et Geomaterialia 7(3), 355–361.

DOLEŽALOVÁ, H., KAJZAR, V., SOUČEK, K., STAŠ, L (2012): Analysis of surface movements from undermining in time. Acta Geodynamica et Geomaterialia 9(3), 389–400.

DOPITA, M. et al. (1997). Geologie české části hornoslezské pánve. Praha: MŽP ČR, Praha, 278p.

FLETCHER, K. (ed.) (2007): InSAR Principles: Guidelines for SAR Interferometry Processing and Interpretation. ESA, Noordwijk.

HANSSEN, R. F. (2001): Radar interferometry: Data interpretation and Error Analysis. Kluwer Academic Publishers, Dordrecht, 328p. http://dx.doi.org/10.1007/0-306-47633-9

KADLEČÍK, P., SCHENK, V., SEIDLOVÁ, Z., SCHENKOVÁ, Z. (2010): Analysis of vertical movements detected by radar interferometry in urban areas. Acta Geodynamica et Geomaterialia 7(3), 371–380.

KAJZAR, V., DOLEŽALOVÁ H., SOUČEK, K., STAŠ, L (2011): Aerial Photogrammetry observation of the subsidence depression near Karviná. Acta Geodynamica et Geomaterialia 8(3), 309–317.

KAJZAR, V. (2012): Modelling the effects of mining of mineral deposits. PhD thesis, VSB – Technical University of Ostrava, 136p.

KAJZAR, V., DOLEŽALOVÁ, H. (2013): Monitoring and analysis of surface changes from undermining. Geoscience Engineering 59(4), 1–10. http://dx.doi.org/10.2478/gse-2014-0062

LAZECKÝ, M., JIRÁNKOVÁ, E. (2013): Optimization of satellite InSAR technoques for monitoring of subsidence in the surroundungs of Karviná mine: Lazy plant. Acta Geodynamica et Geomateriala 10(1), 51–55.

MASSONNET, D., FEIGL, K. L. (1998): Radar interferometry and its application to changes in the Earth's surface. Reviews of Geophysics 36, 441–500. http://dx.doi.org/10.1029/97RG03139

MULKOVÁ, M., POPELKOVÁ, R. (2013): Displays of hard coal deep mining in aerial photos. AUC Geographica 2013(1), 25–39.

PERSKI, Z., JURA, D. (1999): ERS SAR Interferometry for Land Subsidence Detection in Coal Mining Areas. Earth Observation Quarterly 63, 25–29.

SCHENK, J. (2006): Měření pohybů a deformací v poklesové kotlině. VŠB-TU Ostrava, 175p.

SKEEN, J. (2011): TxDOT Survey Manual, http://onlinemanuals.txdot.gov/txdotmanuals/ess/index.htm.

STAŠ, L., KAJZAR, V., DOLEŽALOVÁ H., SOUČEK, K., SMETANOVÁ, L., GEORGIOVSKÁ, L. (2009): GPS monitoring of subsidence depression progress on undermined area. Nowoczesne metody eksploatacji węgla i skał zwięzłych. Kraków, AGH, 99–106.

STOW, R. J., WRIGHT, P. (1997): Mining subsidence land surveying by SAR interferometry, Proceedings of the 3rd ERS Symposium, Florence, Italy. http://earth.esa.int/symposia/papers/

TERRAFIRMA project/ESA-GMES, http://www.terrafirma.eu.com.

WEGMÜLLER, U., STROZZI, T., WERNER, C., WIESMANN, A., SPRECKELS, V., BENECKE, N., WALTER, D. (2007): Monitoring of mining induced surface deformation. Proceedings of First Joint PI symposium of ALOS Data Nodes FOR ALOS Science Program, Kyoto.

WERNER, C., WEGMÜLLER, U., STROZZI, T., WIESMANN, A., SANTORO, M. (2007): PALSAR Multi-Mode Interferometric Processing. Proceedings of First Joint PI symposium of ALOS Data Nodes FOR ALOS Science Program, Kyoto.

RESUMÉ

Měření poklesů z poddolování technikami diferenciální radarové interferometrie a GPS na lokalitě nedaleko Karviné

V české části hornoslezské pánve způsobuje hlubinná těžba uhlí značné změny reliéfu. Přímo člověk upravuje reliéf zejména navážením hlušiny a tvorbou dalších antropogenních tvarů, během těžby i následně po ní pak rekultivacemi postiženého území. Nepřímým důsledkem těžby na povrchu jsou poklesy z poddolování. Poklesová kotlina se vytváří na povrchu nad těženým porubem a postupuje ve směru těžby. Největší úhrny poklesů jsou zaznamenány do jednoho roku od začátku těžby, avšak pokles povrchu může doznívat i několik let.

V rámci projektu ESA GMES Terrafirma, jehož řešitelem byl Ústav struktury a mechaniky hornin AV ČR, v.v.i., bylo zpracováno metodou satelitní diferenciální radarové interferometrie (dInSAR) území části hornoslezské pánve, na české straně zahrnující i oblast současné těžby černého uhlí nedaleko města Karviná. Zpracování snímků PALSAR japonské družice ALOS pro období od února 2007 do května 2008 provedla firma GAMMA Remote Sensing. Výsledky odhalily kolem 20 dynamicky se vyvíjejících poklesových kotlin pro toto období. Pro ověření výsledků a vyhodnocení jejich kvality bylo provedeno srovnání vertikálních hodnot poklesů s měřeními statickou metodou GPS prováděnou pracovníky Ústavu geoniky AV ČR, v.v.i. z Ostravy. Tato měření byla prováděna od listopadu 2006 po dobu šesti let na zhruba 100 bodech v dobývacím prostoru Louky nedaleko zastavěné části města Karviné.

Srovnávanými veličinami byly vertikální pohyby přepočtené ze změn mezi povrchem a satelitem pro každé z pěti zpracovaných období pomocí dInSAR s gridem 20 × 20 m a hodnoty vertikálních pohybů změřených pomocí GPS na všech bodech, jejichž hodnoty byly interpolovány v čase podle dní pořízení použitých satelitních snímků. Z bodových GPS dat byly dále plošnou interpolací vytvořeny mapy poklesů pro celé zkoumané území a taktéž mapy poklesů podle přepočtených dInSAR vertikálních hodnot v místech měřených GPS bodů.

Výsledky srovnání ukázaly relativní shodu pro některé z bodů zejména v místech na okrajích vznikající poklesové kotliny pro všechna časová období. V místech centra poklesové kotliny však hodnoty změřené pomocí GPS v obdobích největších poklesů (40 cm/92 dní ve čtvrtém období) výrazně přesahovaly hodnoty vypočtené pomocí techniky dInSAR. Naopak pomocí plošné interpolace nebylo z map poklesů vždy možné jasně vymezit celkovou oblast poklesu kvůli nedostatku bodů v celé lokalitě. Rozdíly ve srovnávaných vertikálních hodnotách byly způsobeny zejména:

A) rozdílnými daty mezi zpracovávanými snímky a daty GPS měření,
B) kalkulací dInSAR vertikálních hodnot z gridu 20 × 20 m vůči přesným souřadnicím GPS bodů,
C) chybami zpracování dInSAR, zejména chybami filtrování a rozbalení fáze před určením konkrétních hodnot poklesu,
D) chybami měření pomocí GPS.

Provedené srovnání ukázalo na možnost využití těchto dvou technik (i společného monitoringu) pro místa plošných deformací území jako jsou poklesy z poddolování, zejména na plošné vymezení hranic poklesové oblasti. Pro zvýšení kvality výsledků je v místech značných změn reliéfu nutné doplnění o výsledky analýzy dalších dat, a to pomocí leteckých snímků, výškových dat a geomorfologické analýzy území, která je na lokalitě prováděna od roku 2011.

Pavel Kadlečík
Institute of Rock Structure and Mechanics of the AS CR, v.v.i., Prague
V Holešovičkách 41, 182 09 Praha 8, Czech Republic
Charles University in Prague, Faculty of Science, Department of Physical Geography and Geoecology
Albertov 6, 128 43 Praha 2
Czech Republic
E-mail: kadlecik.p@seznam.cz

Zuzana Nekvasilová
Charles University in Prague, Faculty of Science, Institute of Geochemistry, Mineralogy and Mineral Resources
Albertov 6, 128 43 Praha 2
Czech Republic
E-mail: themen@centrum.cz

Vlastimil Kajzar
Institute of Geonics AS CR, v.v.i.
Studentská 1768, 708 00 Ostrava-Poruba
Czech Republic
E-mail: vlastimil.kajzar@ugn.cas.cz

Urs Wegmüller
GAMMA Remote Sensing Research and Consulting AG
Worbstrasse 225, CH-3073 Gümlingen
Switzerland
E-mail: wegmuller@gamma-rs.ch

Doležalová Hana
Institute of Geonics AS CR, v.v.i.
Studentská 1768, 708 00 Ostrava-Poruba
Czech Republic
E-mail: hana.dolezalova@ugn.cas.cz